ISSN: 0975-766X
CODEN: IJPTFI
Available Online through ***Research Article***
www.ijptonline.com

STUDYING CHANGES IN DESIGN AND TECHNOLOGICAL PARAMETERS OF THE GRINDING AND MIXING DEVICES WITH CYLINDRICAL WORKING CHAMBERS DEFORMABLE IN CROSS SECTION

Svetlana Yuryevna Lozovaya, Nikolay Mikhailovich Lozovoy, Valeriy Anatolyevich Uvarov, Lyudmila Vasilyevna Ryadinskaya, Rashid Rizaevich Sharapov

Belgorod State Technological University named after V.G. Shukhov
46 Kostyukov Street, Belgorod 308012, Russian Federation.
Belgorod State Technological University named after V.G. Shukhov
46 Kostyukov Street, Belgorod 308012, Russian Federation.
Belgorod State Technological University named after V.G. Shukhov
46 Kostyukov Street, Belgorod 308012, Russian Federation.
Belgorod State National Research University
85 Pobeda Street, Belgorod 308015, Russia Russian Federation.
Moscow State University of Civil Engineering (National Research University),
26 Yaroslavskoe Shosse, Moscow 129337, Russian Federation.

Received on 14-08-2016 *Accepted on 20-09-2016*

Abstract.

Increased demand in fine powders with a particle size of less than 5 microns; development of formulations of new synthetic materials with special properties; preparation of finished products corresponding to the specified properties with a close grading and a required particle form demand the creation of technologically new principles of grinding and a corresponding design of grinding devices. A number of rheological components in the modified mixtures is added in an amount from 0.05 to 5%; in this case the powders made from initial components are different from each other in their particle size (from fractions of a micron to 5 mm) and their density (from 0.1 g/cm^3 to 4.0 g/cm^3). The high-quality multi-component mixtures and powders with specified characteristics were prepared in the grinding and mixing devices using a deformation mechanism of thin-walled elements organizing a feed motion control. The maximum equivalent stress, principal stresses according to the fourth energy theory, maximum equivalent motion are set, defined and analyzed depending on a wall thickness of the working chamber, as well as the power required to overcome the resistance forces to feed motion is set, defined and analyzed depending on the technical and geometrical parameters of a grinding and mixing device.

Key words: Fine powders, synthetic materials, particle size distribution, grinding principles, rheological components, modified mixtures, grinding and mixing device, deformation mechanism, thin-walled element, feed, deformable chamber, equivalent stress equivalent motion.

Introduction. The reasons stimulating the search for technologically new grinding principles and corresponding design solutions for grinding devices [1] include: an increased demand in fine powders with a particle size of less than 5 microns; production of new synthetic materials with special properties; preparation of finished products corresponding to the specified properties with a close grading and a required particle form. When grinding materials with a lamellar, columnar and other similar structures, the shock impacts lead to the destruction occurred in layers. For example, such materials contain wollastonite [1] that has a microacicular structure and is used as microreinforcing filler in the paint and varnish industry for improving the thixotropy of paints, and during its use the form of wollastonite particles should be close to spherical in order to reduce shrinkage when firing ceramic masses.

Overview of currently existing small-tonnage grinding devices showed the absence of units, in which the motion control of grinding media and various types of feeding on a material to be ground could be possible.

Today, certain types of construction materials [2] can not be prepared either without the use of mixing equipment capable of providing a desired level of mixture homogeneity. A system of "rheological" additives is used to regulate technological properties of the construction mixture compositions, and a variety of components is introduced in a small amount (0.05-0.5%), but their influence on forming properties of the mortar mixtures and solutions is extremely high. They form their own structural net in the aqueous phase or they interact with the dispersed phase and maintain system stability, enhance an antisediment effect, increase system plasticity and provide a necessary level of thixotropic properties [2-4]. Such additives include superplasticizers, thickeners and water retaining additives based on cellulose ethers, starch ethers, polymeric dispersions and additives based on layered silicates.

Recently, modifying additives having a complex composition have been marketed in a finished form. Hence, a mixing unit capable of qualitative mixing and homogenizing powders from the initial components differing from each other in their particle size (from fractions of a micron to 5 mm) and their density (from 0.1 g/cm^3 to 4.0 g/cm^3) is the basic unit for the production cycle of dry mixtures and their components [2].

Analysis of the condition and trends regarding the technological and technical development of fine grinding and/or mixing of materials with different mechanical and physical properties gives grounds to rest these studies on a suggestion - efficiency of grinding and/or mixing can be substantially increased due to an intensified feed motion and elimination of dead zones with an ability to control a particle movement within a working chamber, which will provide a necessary interaction between the feed components and stable achievement of the required quality of a finished product [3].

The scientific idea of the work is to use the deformation mechanism of thin-walled elements (working chamber) in grinding and mixing devices to organize the feed motion control and the control over corresponding grinding and/or mixing of materials that provide an effective process for producing a final product with the specified properties and characteristics (multi-component mixtures, powders with a particle size less than 10 microns, etc.). In addition, providing a possibility to control the grinding and/or mixing process in a grinding and mixing device, simple design, fast and simple readjustment to work with a variety of bulk materials are an important task.

Main part. Using the deformable working chamber as a working body provides a new mechanism of influence on the medium to be processed. In this case, changed rigidity, deformation type and degree and method of housing installation enable to change the nature of influence on a material depending on its properties and required conditions for grinding and/or mixing process. The deformable housing is made from an elastic material (rubber or corded rubber). The operation of housing causes stresses arising from the deforming effects as a result of rollers' impact made on the housing in cross section from the outside by rotating or reciprocating motion [1,5].

The initial data for calculating rational parameters of the grinding and mixing device with a deformable grinding chamber are:

Q - finished product capacity of device, kg/h;

d_0 - initial product particle size, m (for grinding devices);

d_k - finished product particle size, m (for grinding devices).

Specification of the working chamber's volume V_k:

$$V_k = \frac{3Q}{n\rho_m k_b K_z}, \qquad (1)$$

where n is the number of cycles per hour (8-12), recommended values at n=8; K_z=K_{nz};

k_b - time factor of mill operation $k_b = 0{,}8 \div 0{,}9$;

K_z - ball-to-ball space utilization factor, accepted factor $K_z = 0{,}33K_{nz} \div K_{nz}$, recommended factor $K_z = 0{,}8K_{nz} \div K_{nz}$ (calculation is made for the maximum feed of the mill, when 2/3 of the chamber's volume is filled with metal grinding media);

ρ_m - bulk density of the material to be ground and/or mixed, $\rho_m = 1200 \div 2600$ kg/m^3 (for construction fillers, technical ceramics and uralite);

ρ_1 - density of the grinding medium's material, ρ_1 = 7600 kg/m^3 (for metal grinding media).

The radius of the working chamber before its deformation will be determined through the obtained required volume according to (1) at the degree of deformation $\Delta = 0{,}25$ (most appropriate); values for other cases of deformation are shown in Table 1.

$$R = \sqrt[3]{\frac{V_k}{23{,}9}}, \qquad (2)$$

The length L and radius R of the chamber before its deformation are connected by the relation defined experimentally [1]:

$$L = (4-5)R \approx 5R. \qquad (3)$$

The relationship between the parameters of the housing's elliptic part and the radius of the circumference defining is determined as follows:

$$b = \Delta R; \qquad (4)$$

$$a = \frac{2R + \sqrt{4R^2 - 3b^2}}{3}, \qquad (5)$$

where a, b are major and minor semiaxes of a deformable chamber.

The recommended minimum size of the grinding media d_1 depending on the particle size of the initial product:

$$d_1 = 3d_0. \qquad (6)$$

Table 1. Relationship between v, V_K and Δ.

Δ	v	V_K	R
0.95	0.864	29.9 R^3	$\sqrt[3]{\frac{V}{29{,}9}}$
0.9	0.771	28.3 R^3	$\sqrt[3]{\frac{V}{28{,}3}}$
0.85	0.684	26.9 R^3	$\sqrt[3]{\frac{V}{26{,}9}}$
0.8	0.597	24.7 R^3	$\sqrt[3]{\frac{V}{24{,}7}}$
0.75	0.558	23.9 R^3	$\sqrt[3]{\frac{V}{23{,}9}}$
0.72	Loss of balance		

Define a total number of grinding media for a cylindrical working chamber. Then a total number of grinding media throughout the entire cylindrical chamber will be equal to the sum in each coaxial cylinder, and it will be defined by following equations:

$$N_z = \frac{\pi L}{2r_1}\sum_{i=1}^{K_z}\frac{(R - ir_1)}{r_1} = \frac{\pi}{2}\frac{L}{r_1}\sum_{i=1}^{K_z}\left(\frac{R}{r_1} - i\right); \qquad (7)$$

where $K_z = \left[\frac{R}{2r_1}\right]$ is a number of coaxial cylinders determined by an integer part of the equation;

r_1 is a radius of grinding media.

Then

$$\nu = \frac{4N\pi r_1^3}{3V_k}; \qquad (8)$$

$$\rho = \nu\rho_1 + (1-\nu)\rho_m, \qquad (9)$$

where $(1-\nu) = K_{\Pi 3}$ is a factor of useful material filling of the working chamber's ball-to-ball space (for mills).

Specify a wall thickness of chamber δ, and for the cameras deformable in cross section by reciprocating motion.

Check the conditions:

. (10)

$$\alpha = \frac{a}{a+\delta} < 1; \text{ или } \alpha = \frac{b}{b+\delta} < 1; \qquad (11)$$

или	or

Define a resistance moment in torsion of bars with elliptical cross section W_K:

$$W_K = \frac{\pi}{2}(b+\delta)^3\left(1-\alpha^4\right)m; \qquad (12)$$

Further specify an estimated external torque M_K:

$$M_K = \frac{F_{TR}}{2} = \frac{a^3 bL\omega^2\rho}{2}, \qquad (13)$$

then according to the fourth energy theory [8-10]:

$$\sigma_{IV} = \sqrt{3}\frac{M_K}{W_K} = [\sigma], \qquad (14)$$

where $[\sigma]$ is a permissible normal stress.

The requirement (14) will be observed if:

$$\delta \geq [\delta], \qquad (15)$$

where δ is an actual or design wall thickness of the housing.

Figure 1 presents the torque and chamber wall thickness based graphs of variation of the maximum equivalent stress. The analysis shows that at a fixed frequency of the drive rotation the equivalent stress increases with a decreased chamber wall thickness, i.e. it is described with an inverse relationship. And at a fixed chamber wall thickness, the equivalent stress increases with higher frequency of the drive rotation. The extreme left points on the curves correspond to the minimum permissible chamber wall thickness.

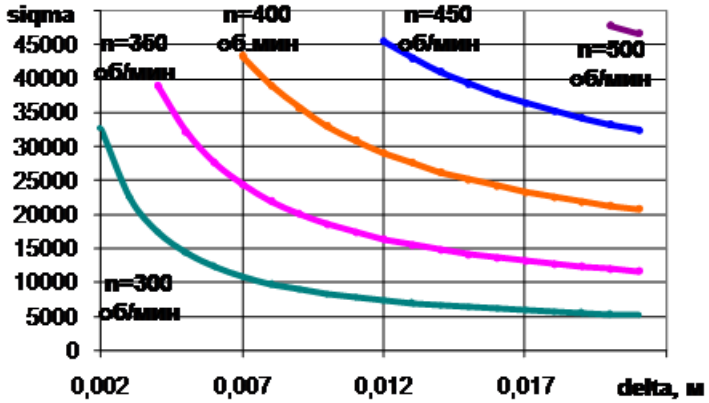

delta, м	delta, m
об/мин	rpm

Figure 1. Relationships between the maximum equivalent stresses emerging under the influence of torque and the chamber wall thickness (R=0.1 m; L=0.4 m) at different values of the drive rotation frequency

When deforming, the working chamber's main property is the ability to change its dimensions under load [3-4, 6-8]. The output parameter of any deformable element is a motion transmitted to a processed material. The motion is characterized by a change in the position of a deformable element's fixed point as such element moves relative to the reference point. Therefore, the deformable grinding chamber's force calculation is based on calculation of the housing's strength. To do this, the estimated linear load on the chamber should be determined:

$$q = \frac{\rho_m(1-\nu)+\rho_1\nu}{L}. \qquad (16)$$

Let us calculate the radius R_{1c} of the undeformed housing's middle surface:

$$R_{1c} = R + \frac{\delta}{2}. \qquad (17)$$

Let us calculate the constants $C_1\left(\frac{кг}{м}\right)$; $C_2\left(\frac{кг}{м}\right)$ and $C_3\ (кг)$ in accordance with the equations [6-7].

$$C_1 = \frac{\frac{q}{2}\left[\frac{L^2}{R_{1c}}(1+\mu) - \frac{L^4}{12R_{1c}^3} - R_{1c}\left(1-\mu^2\right)\right]}{L\left(\frac{L^2}{3R_{1c}^2} - \frac{3}{2}\mu - 2\right)}; \qquad (18)$$

$$C_2 = \mu\frac{q}{2} + \frac{1}{R_{1c}}\left(\frac{qL^2}{2R_{1c}} + C_1\frac{L}{2}\right); \qquad (19)$$

$$C_3 = \frac{qR_{1c}}{2} + \mu C_2 R_{1c}, \qquad (20)$$

where μ is Poisson's ratio of the working chamber's material, $\mu = 0{,}5$.

Let us define the axial N_x and ring N_θ strength at point B of the middle surface on the lower half of the housing for the cross sections $2-2$ and $3-3$ (Fig. 2).

For the section $2-2$ ($x = 0$, $\theta = 0$):

$$\overline{N}_{\theta B}^{2-2} = \frac{q}{2}; \qquad (21)$$

$$\overline{N}_{xB}^{2-2} = C_2. \qquad (22)$$

For the section $3-3$ ($x = \frac{L}{2}$, $\theta = 0$), the same equations should be used:

$$\overline{N}_{\theta B}^{3-3} = \frac{q}{2}; \qquad (23)$$

$$\overline{N}_{xB}^{3-3} = C_2 - \frac{L}{2R_{1c}}\left(\frac{q}{8} + C_1\right). \qquad (24)$$

Let us calculate the principal stresses for points B, B' of the cross sections $2'-2$ and $3'-3$ of the housing (Fig. 1).

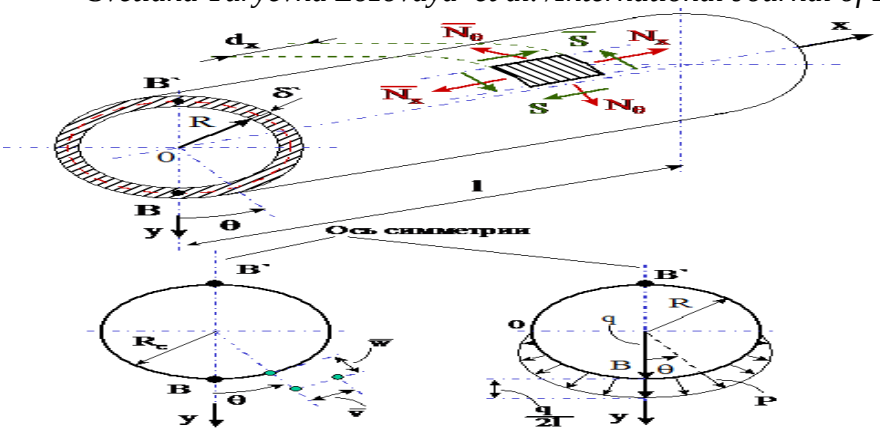

Figure 2. Calculation model

Ось симметрии	Axis of symmetry

For point B of section $2-2$ ($\theta = 0$):

$$\sigma_{1B}^{2-2} = \frac{\overline{N}_{xB}^{2-2}}{\delta} - \frac{qL^2}{12\pi R_{1c}^3 \delta}; \qquad (25)$$

$$\sigma_{2B}^{2-2} = \frac{\overline{N}_{\theta B}^{2-2}}{\delta} > 0. \qquad (26)$$

For point B' of section $2-2$ ($\theta = \pi$):

$$\sigma_{1B'}^{2-2} = \frac{qL^2}{12\pi R_{1c}^3 \delta}; \qquad (27)$$

$$\sigma_{2B'}^{2-2} = 0. \qquad (28)$$

For point B of section $3-3$ ($\theta = 0$):

$$\sigma_{1B}^{3-3} = \frac{\overline{N}_{xB}^{3-3}}{\delta} + \frac{qL^2}{12\pi R_{1c}^3 \delta}; \qquad (29)$$

$$\sigma_{2B}^{3-3} = \frac{\overline{N}_{\theta B}^{3-3}}{\delta} > 0. \qquad (30)$$

For point B' of section $3-3$ ($\theta = \pi$):

$$\sigma_{1B'}^{3-3} = -\frac{qL^2}{12\pi R_{1c}^3 \delta}; \qquad (31)$$

$$\sigma_{2B'}^{3-3} = 0. \qquad (32)$$

Let us define the estimated equivalent stresses σ_{IV} for sections $2'–2$, $3'–3$ and identify a critical point of the chamber's middle surface:

$$\sigma_{IVB}^{2-2} = \sqrt{\left(\sigma_{1B}^{2-2}\right)^2 + \left(\sigma_{2B}^{2-2}\right)^2 - \sigma_{1B}^{2-2}\sigma_{2B}^{2-2}}\,; \qquad (33)$$

$$\sigma_{IVB'}^{2-2} = \sqrt{\left(\sigma_{1B'}^{2-2}\right)^2 + \left(\sigma_{2B'}^{2-2}\right)^2 - \sigma_{1B'}^{2-2}\sigma_{2B'}^{2-2}}\,; \qquad (34)$$

$$\sigma_{IVB}^{3-3} = \sqrt{\left(\sigma_{1B}^{3-3}\right)^2 + \left(\sigma_{2B}^{3-3}\right)^2 - \sigma_{1B}^{3-3}\sigma_{2B}^{3-3}}\,; \qquad (35)$$

$$\sigma_{IVB'}^{3-3} = \sqrt{\left(\sigma_{1B'}^{3-3}\right)^2 + \left(\sigma_{2B'}^{3-3}\right)^2 - \sigma_{1B'}^{3-3}\sigma_{2B'}^{3-3}}\,. \qquad (36)$$

Critical or the most stressful point will be the point, for which

$$\sigma_{IV} = \sigma_{IV\max}, \qquad (37)$$

among four obtained values in (33)-(36).

The strength of the housing is checked by the condition:

$$\sigma_{IV\max} \le [\sigma]. \qquad (38)$$

If the regulatory requirement (38) is not satisfied, i.e. $\sigma_{IV\max} > [\sigma]$ with excessive stress over 5 per cent:

$$\frac{\sigma_{IV\max} - [\sigma]}{[\sigma]} 100\% > 5\%, \qquad (39)$$

it is necessary to structurally enlarge the size δ, and verify again whether the condition of the relationship (38) has been observed.

Figure 3 shows the principal stress graphs for points B, B' in sections 2-2, 3-3 depending on the chamber wall thickness. All graphs are of the same type and demonstrate that the stresses and the chamber wall thickness have an inverse relationship. S1B3 line shows that the longitudinal stress is maximum (critical point) at point B in section 3-3; the plus sign indicates that the considered point sees tensile deformation, at point B' (S1B'3 line) stresses are about twice less, and the minus sign indicates that point B' has tensile deformation.

With an increased chamber wall thickness in section 3-3 at point B, the stresses are four orders less, and they increase by three orders of magnitude at point B'. S1B2, S1B'2 lines represent changes of longitudinal stresses in section 2-2, they are about 3 times less than the stresses at the critical point. S2B3, S2B'3, S2B2, S2B'2 lines indicate the change

in stresses due to the ring strength. The ring stresses are not available for point B' in section 2-2, 3-3, and they are approximately 20 times less than the longitudinal ones for point B.

If the maximum equivalent stresses arising under the action of torque and the maximum stress (longitudinal stress arising from the feed weight in the absence of compression, when the cross section is a circle) are compared at critical point B, the stress arising out of torque is 3-5 times more than the stress arising out of feed weight depending on frequency of the drive rotation (Fig. 2).

The maximum radial motion w_{MAX} of the housing wall is defined by the formula:

$$w_* = \frac{qR_{1c}}{2} + \mu\left[\left(\frac{qL^2}{16R_{1c}} + C_1\frac{l}{2}\right) + C_2R_{1c}\mu\right] - 2(1+\mu)\left(\frac{qL^2}{16R_{1c}} + C_1\frac{L}{2}\right) +$$

$$+\frac{1}{R_{1c}}\left[-\frac{1}{R_{1c}}\left(\frac{qL^4}{768R_{1c}} + C_1\frac{L^3}{48}\right) + C_2\frac{L^2}{8} - \mu\frac{qL^2}{16}\right] + C_3 + \frac{qL^4}{384R_{1c}^3\pi}; \qquad (40)$$

$$w_{MAX} = \frac{w_*}{E\delta}. \qquad (41)$$

Where $E \approx 10\ МП, \quad \sigma_p \approx 38000\ кг/см^2.$

10 МП	10 MPa
кг/см^2	kg/cm^2
σ_p	σ_r

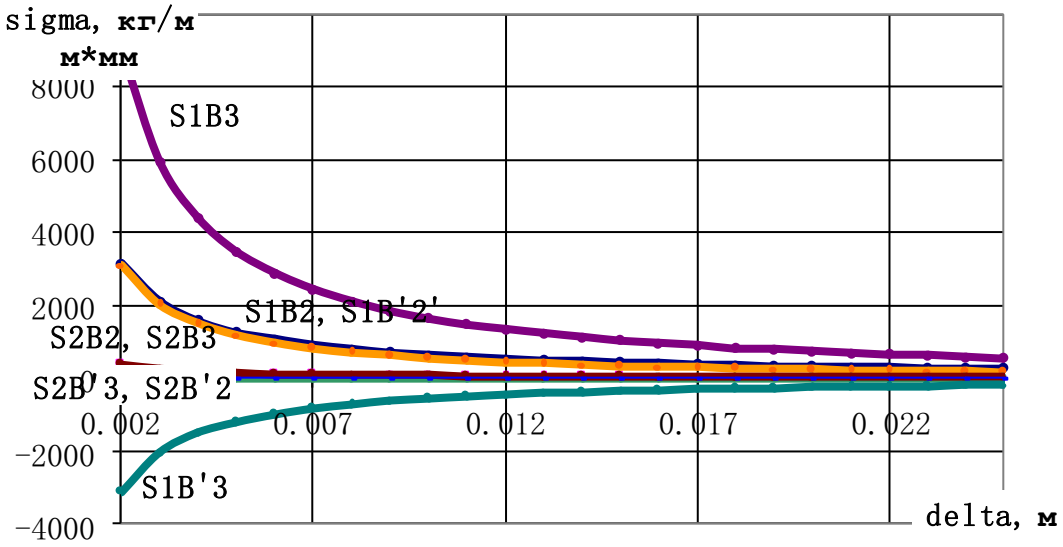

кг/мм*мм	kg/mm*mm
delta, м	delta, m

Figure 3. Feed weight based principal stresses for points B, B' in sections 2-2, 3-3 and the chamber wall thickness (R=0.1 m; L=0.4 m) dependency diagram.

Figure 4 shows dependency diagrams of the chamber wall thickness based equivalent stresses σ_{IV} calculated according to the forth energy theory for sections 2-2, 3-3 and arising under the feed weight and torque. They indicate that the chamber is loaded as much as possible at point B (critical point) in section 3-3. The change in stresses is inversely proportional, i.e. stresses decrease with an increased thickness of the chamber wall. The equivalent stresses for point B' in section 3-3 and 2-2 and for point B in section 2-2 are approximately equal and 3 times less than the equivalent stress at the critical point.

The maximum dip in the curve (Figure 4, b) depending on the thickness of the chamber wall is also inversely proportional.

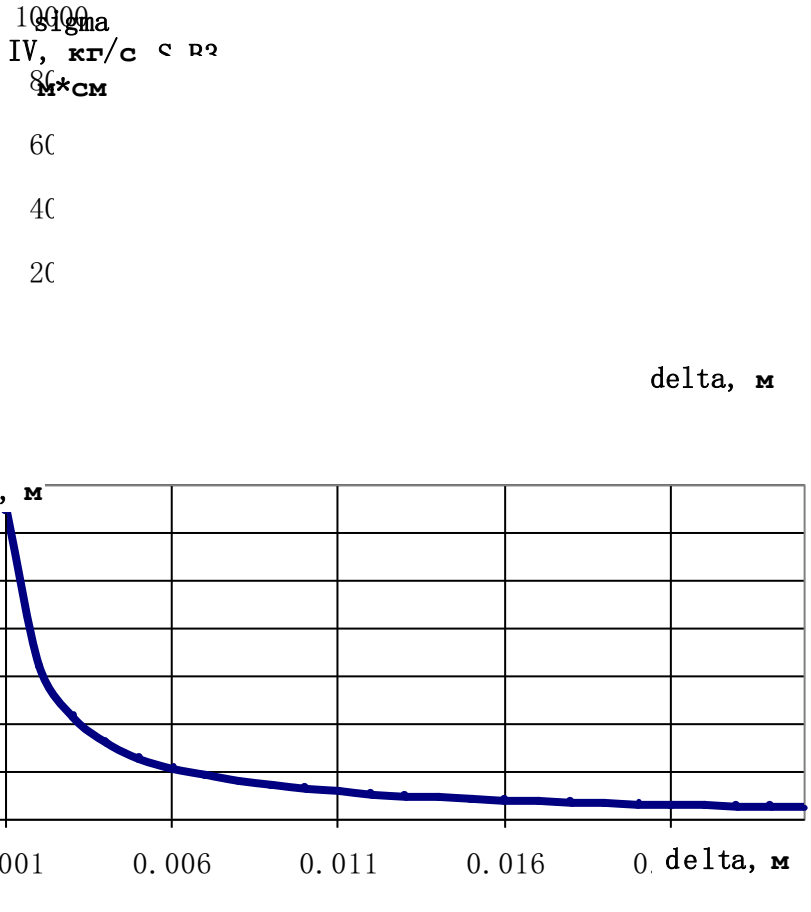

кг/см*см	kg/cm*cm
delta, м	delta, m
а)	a)
б)	b)

Figure 4. Estimated relationships: a - dependency diagrams of the chamber wall thickness based estimated equivalent stresses σ_{IV} arising under the torque and feed weight for sections 2-2, 3-3; b – maximum dip in the curve and chamber wall thickness (R=0.1 m; L=0.4 m) relationship.

The amount of energy required for grinding and/or mixing of the material to a certain size depends on the physico-mechanical properties of the material, type and condition of the device's working surfaces, such as the power unit,

drive kinematics, geometric and technological parameters of the device. Therefore, to determine the analytical relationship between the energy consumption and the process of grinding and/or mixing, the principles of continuum mechanics have been used.

The power spent on overcoming the resistance forces for devices deformable in cross section:

- by rotating motion

$$P_n \approx \pi^2 \frac{f_n^2}{3}(1-f_n)^2(1-\varepsilon^2)\rho\omega^3 a^4 L;$$

$$P_\tau = \frac{\pi f_\tau}{4}\rho\omega^3\left(R-\frac{d_1}{2}\right)^2 d_1^3\left[\frac{\pi(2R-d_1)}{d_1}\right]\left[\frac{L}{d_1}\right]; \qquad (42)$$

$$P_e \approx \frac{4}{3}\pi^2 f_e^2\left(1+\left(\frac{1-f_e}{2}\right)^2\right)^2(1-\varepsilon^2)\rho\omega^3 a^4 L;$$

$$P_\Sigma = (P_n + P_\tau + P_e)/\eta, \qquad (43)$$

where η is an efficiency factor of the drive used for deformation $\eta = 0{,}7\ldots0{,}85$

f_n, $f_e = 0{,}015$; $f_\tau = 0{,}08$ factors of friction between the feed material and the feed and chamber material, respectively;

$\omega = (31{,}4\ldots52{,}4)/10; 1/c$ - angular rate of feed.

Figure 5 displays dependency diagrams of the power spent on overcoming the resistance forces to feed motion and the frequency of the drive rotation for various standard sizes of working chambers. The amount of power spent on overcoming the forces F_n, F_e is roughly equal in value for each standard size of working chambers, and on overcoming the force F_τ - about two orders of magnitude higher; this can be explained by the fact that the feed rate in the wall area is higher, i.e. when deforming the chamber walls carry a mixture of grinding media and material.

- by reciprocating motion:

$$P_n \approx \frac{32}{9}\pi^2 f_n^2(1-f_n)^2(1-\varepsilon^2)\rho\omega^3 a^4 L;$$

$$P_\tau \approx \frac{f_\tau}{3}\omega^3\rho LR\left(d_1^3(2\pi-\alpha^M)+3Rd_1^2\left((2\pi-\alpha^M)-\frac{\varepsilon^2}{2}\left(\frac{1}{4}\sin 4\alpha^M+\pi-\frac{\alpha^M}{2}\right)\right)\right); \qquad (44)$$

$$P_e \approx \frac{4}{3}\pi^2 f_e^2\left(1+\left(\frac{1-f_e}{2}\right)^2\right)^2(1-\varepsilon^2)\rho\omega^3 a^4 L.$$

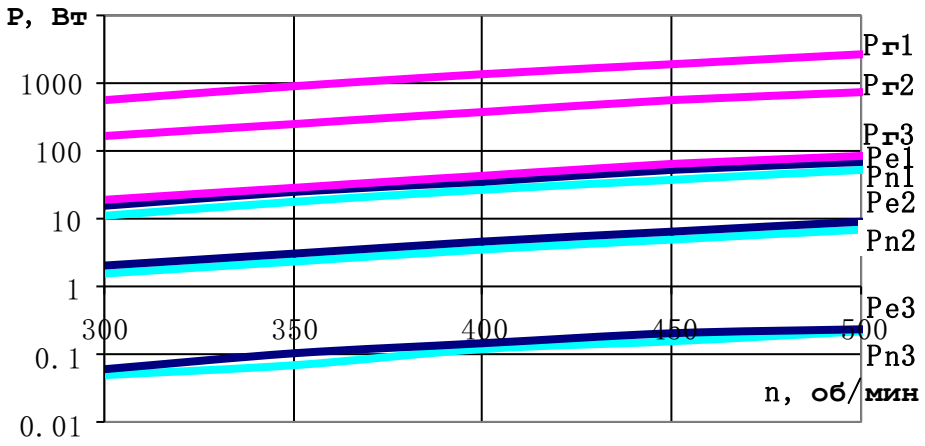

P, Вт	P, W
n, об/мин	n, rpm

Figure 5. Dependency diagrams of the power spent on overcoming the resistance forces to feed motion and the frequency of the drive rotation for various standard sizes of working chambers (1 – R=0.15 m; L=0.6 m; 2 - R=0.1 m; L=0.4 m; 3 - R=0.05 ; L=0.2).

Figure 6 displays dependency diagrams of the power spent on overcoming the resistance forces to feed motion and the frequency of the drive rotation for various standard sizes of working chambers. They show that the value of the power spent on overcoming the resistance forces to the same order feed motion for each standard size of the working chamber, but P_τ is slightly higher than P_n and P_e, which are approximately equal in magnitude.

The design parameters of the drive, motor type and power are selected according to the known methods [5].

Summary. Fine powders with a particle size of less than 5 microns and high-quality multi-component mixtures with specified characteristics can be prepared in the grinding and mixing equipment using a deformation mechanism of thin-walled elements organizing a feed motion control. The maximum equivalent stress, principal stresses according to the forth energy theory, maximum equivalent motion are set, defined and analyzed depending on a wall thickness of the working chamber, as well as the power required to overcome the resistance forces to feed motion is set, defined and analyzed depending on the technical and geometrical parameters of a grinding and mixing device.

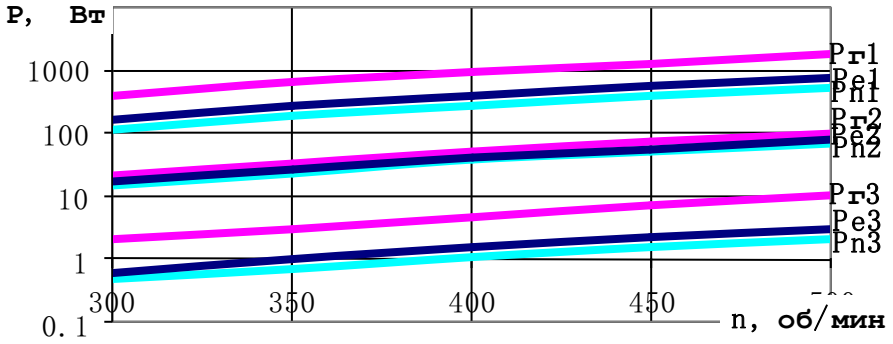

P, Вт	P, W
n, об/мин	n, rpm

Figure 6. Dependency diagrams of the power spent on overcoming the resistance forces to feed motion and the frequency of the drive rotation for various standard sizes of working chambers (1 – R=0.15 m; L=0.6 m; 2 - R=0.1 m; L=0.4 m; 3 - R=0.05 ; L=0.2)

Conclusions.

1. Equations are obtained to determine stresses arising out of torque, a feed weight, as well as a relationship between the chamber's deformation and the total stress calculated according to the forth energy theory for a cylindrical chamber deformable in cross section by rotating and reciprocating motion; they indicate that:

a) At a fixed frequency of the drive rotation the equivalent stresses increase with a decreased chamber wall thickness, i.e. they are described with an inverse relationship.

b) The feed weight based principal stresses are of the same type and demonstrate that the stresses and the chamber wall thickness have an inverse relationship. The longitudinal stress at the critical point located on the vertical axis of symmetry on the bottom of the chamber is about 3 times higher than the stresses arising in the chamber material at the places where the chamber is fixed on the trunnions. The stresses due to the ring strength at the critical point are approximately 20 times less than the longitudinal ones.

c) The maximum stresses arising under the action of torque at the critical point, increase, at higher frequency of the drive rotation in 1.7 times, in 5 times compared with the maximum stresses arising out of the feed weight in the absence of chamber's deformation when the cross section is a circle.

d) Depending on the chamber wall thickness, the values of estimated equivalent stresses calculated according to the forth energy theory and arising under the action of feed weight and torque show that change in stresses is inversely proportional and the stresses arising in the chamber material at the places where the chamber is fixed on the trunnions are about 3 times less than the equivalent stress at the critical point.

2. For the schemes of deformation in cross section by rotating motion, it has been found that the values of power spent on overcoming the forces F_n, F_e are roughly equal in value for each standard size of working chambers, and the power P_τ spent on overcoming the force F_τ is about two orders of magnitude higher; this can be explained by the fact that the feed rate in the wall area is higher, i.e. when deforming the chamber walls carry a mixture of grinding media and material.

3. For the schemes of deformation in cross section by reciprocating motion, it has been revealed that values of the power spent on overcoming the resistance forces to the same order feed motion are roughly equal in value for each standard size of the working chamber, but P_τ is about 5 times higher than P_n, and the values P_n and P_e are approximately equal in magnitude.

References

1. Lozovaya S.Yu., 2004. Some findings of grinding process in the mill equipped with a grinding chamber deformable in cross section by rotation. Ivanovo: Proceedings of Universities "Chemistry and Chemical Technology", Volume 47(8), pp. 138-140.
2. Lozovaya S.Yu., Lozovoy N.M. and Shirina N.V., 2013. Influence of Processing Characteristics of Mixer with the Changing Camera on Quality of Heat-Insulating Plasters on the Basis of Modifying Agent and Anthropogenic Raw Materials, World Applied Sciences Journal, Volume 24(10), pp. 1404-1410.
3. Cheng S., Zhang J., Zhang Z. and Han B., 2007. Novel micro emulsions: ionic liquid-in-ionic liquid. Chem. Comm, Issue 24, pp. 2497–2499.
4. Demin E.N., 2011. Cast-in-situ refractory articles and dry concrete mixes with additions of caked chromoalumina spinel. Refractories and Industrial Ceramics, Volume 51(6), pp. 419-420.
5. Lozovaya S.Yu., Riadinskaya L.V. and Sablin V.S., 2014. Theoretical Bases of the Calculation of the Energy, which it Spends for the Process of Materials Grinding in Accordance with Geometrical and Technological Characteristics of the Chamber of the Barrel-Shaped Form, International Journal of Applied Engineering Research, Volume 9(22), pp. 16891-16902.
6. Lozovaya S.Yu. and Abdeev B.M., 2004. Estimation of the maximum deformability of the working chambers loaded in cross section. "Building and Road Machines", Issue 11, pp. 35-38.
7. Lozovaya S.Yu., Lozovoy N.M. and Abdeev B.M., 1993. Modeling of a stress state of a material of a variable working chamber of the mixer depending on the technological eccentricity, 2014. World Applied Sciences Journal, Volume 30(8), pp. 983-989.
8. Vishnevskiy A., Krylov A., Krasnov I. and Lapovok A., 1993. Calculation of static magnetization for thin-walled constructions by boundary element method. IEEE Transactions on Magnetics, Volume 29(4), pp. 2152 – 2155.
9. Geir A. and Gunnlaugsson P., 1982. A finite element formulation for beams with thin walled cross-sections. Computers and Structures, Volume 15(6), pp. 691-699.